Environmental Science & Technology

Article

pubs.acs.org/est

# Cysteine-Induced Modifications of Zero-valent Silver Nanomaterials: Implications for Particle Surface Chemistry, Aggregation, Dissolution, and Silver Speciation

Andreas P. Gondikas,[†,§] Amanda Morris,[†,§] Brian C. Reinsch,[‡,§] Stella M. Marinakos,[§] Gregory V. Lowry,[‡,§] and Heileen Hsu-Kim*[,†,§]

[†]Department of Civil and Environmental Engineering, Duke University, Box 90287, Durham, North Carolina 27708, United States

[‡]Department of Civil and Environmental Engineering, Carnegie Mellon University, Pittsburgh, Pennsylvania 15213, United States

[§]Center for the Environmental Implications of NanoTechnology (CEINT), P.O. Box 90287, Durham, North Carolina 27708, United States

Supporting Information

**ABSTRACT:** The persistence of silver nanoparticles in aquatic environments and their subsequent impact on organisms depends on key transformation processes, which include aggregation, dissolution, and surface modifications by metal-complexing ligands. Here, we studied how cysteine, an amino acid representative of thiol ligands that bind monovalent silver, can alter the surface chemistry, aggregation, and dissolution of zero-valent silver nanoparticles. We compared nanoparticles synthesized with two coatings, citrate and polyvinylpirrolidone (PVP), and prepared nanoparticle suspensions (approximately 8 $\mu$M total Ag) containing an excess of cysteine (400 $\mu$M). Within 48 h, up to 47% of the silver had dissolved, as indicated by filtration of the samples with a 0.025-$\mu$m filter. Initial dissolution rates were calculated from the increase of dissolved silver concentration when particles were exposed to cysteine and normalized to the available surface area of nanoparticles in solution. In general, the rates of dissolution were almost 3 times faster for citrate-coated nanoparticles relative to PVP-coated nanoparticles. Rates tended to be slower in solutions with higher ionic strength in which the nanoparticles were aggregating. X-ray absorption spectroscopy analysis of the particles suggested that cysteine adsorbed to silver nanoparticles surfaces through the formation of Ag(+I)—sulfhydryl bonds. Overall, the results of this study highlight the importance of modifications by sulfhydryl-containing ligands that can drastically influence the long-term reactivity of silver nanoparticles in the aquatic environment and their bioavailability to exposed organisms. Our findings demonstrate the need to consider multiple interlinked transformation processes when assessing the bioavailability, environmental risks, and safety of nanoparticles, particularly in the presence of metal-binding ligands.

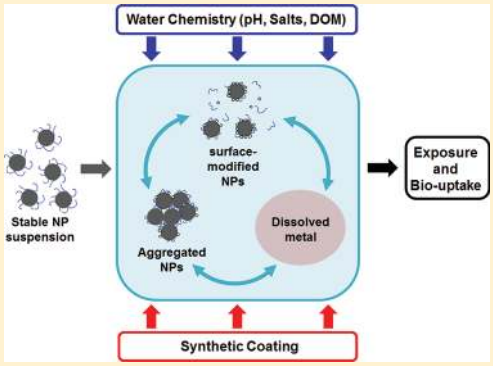


## INTRODUCTION

The wide use of silver nanoparticles (Ag NPs) in commercial products has recently gained much attention due to the potential toxic effects resulting from their unintended release into the environment.[1,2] The reactivity and transport of Ag NPs in the aquatic environment will depend on key transformation processes, which include aggregation, dissolution, and surface modifications by metal-complexing ligands. These processes work in synergistic or antagonistic ways to influence the lifetime of nanoparticles in the environment and the bioavailability of silver to exposed organisms. For example, adsorption or desorption of organic matter or metal-binding ligands will modify the surface of nanoparticles. Ionic compounds or long-chain moieties can induce surface charge or steric effects that influence particle coagulation and settling kinetics.[3−5] Aggregation can lead to changes in reaction rates (such as dissolution and sorption) by decreasing the surface area that is exposed to bulk solution.[6−8] Dissolution of nanoparticles will in turn decrease the size of the particles and increase dissolved metal concentration in water, which subsequently affects ligand adsorption and desorption kinetics.

In natural waters Ag(+I) is expected to form strong bonds with ligands such as chloride, sulfide, and other forms of reduced sulfur (e.g., organic thiols).[9,10] Ag(+I) is capable of forming relatively insoluble mineral phases (e.g., $Ag_2S$, AgCl) that can serve as terminal fates for monovalent silver in freshwater, wastewater, and seawater.[11−14] Recent studies showed that Ag NPs dissolve very slowly in water,[15] but oxidative dissolution is faster in sulfide- and chloride-rich

Special Issue: Transformations of Nanoparticles in the Environment

Received: January 15, 2012
Revised: March 16, 2012
Accepted: March 26, 2012
Published: March 26, 2012

   dx.doi.org/10.1021/es3001757 | Environ. Sci. Technol. 2012, 46, 7037−7045

environments.[16−19] In waters rich with organic matter, sulfhydryl-containing organic compounds (thiols) may compete with inorganic ligands and increase dissolved silver concentration.[20] Hence, thiols have the potential to play a key role for the environmental fate of Ag NPs.

In natural waters thiols tend to be associated with low molecular weight organic ligands and with humic substances. In sediments and water, thiols are typically present in nanomolar to micromolar concentrations, depending on environmental conditions such as redox potential, the presence of organisms that actively excrete thiol-containing compounds, and other metals that may catalyze the oxidation of thiols.[21−25] In addition, thiol-containing biomolecules are abundant in biological media such as bacterial plasma, tissues, and blood.[26,27]

Hydrophilic thiols of low molecular weight (such as glutathione, mercaptoacetate, and cysteine) are known to decrease the aggregation and precipitation rates of metal-sulfide nanoparticles by adsorbing to their surface and changing the particle surface charge.[5,8,29] Cysteine (CYS) has also been used in Ag NP toxicity studies to chelate dissolved silver ions.[30−32] Some of these studies noted that cysteine increased the dissolution of silver and slowed aggregation of Ag NPs; however, these phenomena were not studied in detail.[30,31] To predict and understand Ag NP toxicity to organisms, we need to identify the physicochemical processes that these particles undergo in the presence of ligands, and particularly thiol-containing ligands such as cysteine.[33]

The goal of this study was to better define the effect of low molecular weight thiols such as cysteine on Ag NP behavior and speciation in aquatic settings. Aqueous suspensions of metallic Ag NPs were exposed to dissolved cysteine, and the dissolution, aggregation, and surface modifications of the nanoparticles were monitored. We compared cysteine reactivity to Ag NPs manufactured with two common types of synthetic coatings: citrate and polyvinylpirrolidone (PVP), which may influence the available reactive surface area on the nanoparticles. Cysteine was selected because of this amino acid's well-defined structure (relative to humic macromolecules) and because cysteine is widely used in Ag NPs toxicity experiments to assess the effects of dissolved $Ag^+$. In addition, we used X-ray absorption near edge spectroscopy (XANES) to study the speciation of silver in Ag NPs following exposure to cysteine.

## MATERIALS AND METHODS

**Ag NP Synthesis and Characterization.** Synthesis of zero-valent silver nanoparticles with citrate and PVP (55 kDa molecular weight) coatings (hereafter referred to as Ag-CIT and Ag-PVP, respectively) followed previously published methods.[34,35] Particle monomer size was characterized with transmission electron microscopy (TEM) (Figure S1 in Supporting Information). Number-based size distributions of the two nanomaterials were estimated from the TEM images by counting the number of particles, sorting them into 5-nm or 2-nm size intervals, and plotting the counts in histograms (Figure S1). All samples containing the Ag-CIT nanoparticles were prepared in plastic containers and cuvettes, while Ag-PVP samples were prepared in glass containers (due to loss of PVP-coated nanoparticles on the walls of plastic containers).

Ag-CIT primarily consisted of spherical particles with some oval-shaped particles. The average geometric diameter was 19.1 ± 12.7 nm ($n$ = 188). Ag-PVP consisted of spherical particles with average geometric diameter of 7.6 ± 2.0 nm ($n$ = 106). The specific surface areas (SSA) of the Ag NPs were estimated by summing the surface area of each particle counted for the size distribution (assuming spherical geometry) and dividing by the total mass of particles:

$$\mathrm{SSA} = \frac{\sum_i (\pi \times d_i^2)}{\rho \times \sum_i \left(\frac{\pi \times d_i^3}{6}\right)} \quad (1)$$

In eq 1, $i$ refers to each individual particle in the TEM images, $d_i$ is the diameter of particle $i$, and $\rho$ the density of metallic silver (10.50 g/mL[36]). The error of the diameter measurements was calculated based on the resolution of the TEM images (see Supporting Information). From eq 1, we calculated SSA to be 16.1 ± 4.5 $m^2/g$ for Ag-CIT and 66.1 ± 7.0 $m^2/g$ for Ag-PVP.

**Exposure of Ag NP to Cysteine.** Stock solutions of approximately 8 mM cysteine were prepared in degassed water, stored at 4 °C, and utilized within two weeks of preparation. All nanoparticle dissolution and aggregation experiments were performed with a buffer solution consisting of 7 mM sodium bicarbonate (Fisher Scientific, Pittsburgh, PA) adjusted to pH 7.5, 10−500 mM $NaNO_3$, and 400 $\mu$M cysteine. Experiments were initiated by diluting an aliquot of silver nanoparticle stock suspension in the buffer solution. A selection of control solutions included Ag NPs suspended in the bicarbonate buffer without cysteine or with 400 $\mu$M serine instead of cysteine. The samples were stored capped and at room temperature in our laboratory. No additional precautions were taken to protect suspensions from laboratory light. Serine and cysteine are structurally analogous in that serine has a hydroxyl group where cysteine has a thiol group. Particle concentrations in all treatments corresponded to 7.6−8 $\mu$M total silver.

**Quantification of Dissolved Silver and Cysteine.** Each mixture of Ag NPs was produced in 6−14 replicates. Dissolved silver and cysteine concentrations were measured 20 min to 48 h after preparation. For each time point, two replicates were "sacrificed" for filtration with 0.025-$\mu$m membrane filters (VSWP Millipore) fitted on a glass vacuum filtration apparatus. Before filtering the suspensions, the membranes were primed with 10 mL of a solution containing 7.5 mM $NaHCO_3$ at pH 7.5. This solution was passed through the filter and then discarded prior to filtering sample suspensions. Dissolved silver was nominally defined as the silver concentration in the filtrate, which was quantified with inductively coupled plasma mass spectroscopy (Agilent Technologies, Santa Clara, CA) after acidifying the filtered samples with 2% $HNO_3$ and 1% HCl.

The concentration of cysteine in aliquots of the filtered samples was quantified using a previously described method[37,38] that employed derivatization of CYS, separation with reverse-phase high-performance liquid chromatography, and detection by UV absorbance.

Control experiments were performed to confirm that dissolved Ag−CYS complexes, $Ag^+$, and free CYS were able to pass through the filters. In these experiments, we prepared three control solutions: (1) 9.3 $\mu$M $AgNO_3$ + 400 $\mu$M CYS (pH 7.5, 10 mM $NaNO_3$); (2) 1.9 $\mu$M $AgNO_3$ (pH 8.3); and (3) 100 $\mu$M CYS alone (pH 7.3, 10 mM $NaNO_3$). These mixtures were filtered through the 0.025-$\mu$m membrane filters. The recovery of silver in filtrates of the $AgNO_3$ and $AgNO_3$+CYS mixtures were 94.1% and 92.1%, respectively. The percentage of total CYS quantified in the filtrate was 92% in the CYS-only mixture and 90% in the $AgNO_3$+CYS mixture.

The removal efficiency of nanoparticles by the filtration system was tested by quantifying the retention of silver after

filtration of Ag NP stock solutions. Less than 0.3% (±0.05) and 11% (±0.5) of the total silver were recovered after filtration from Ag-CIT and Ag-PVP stock suspensions, respectively, indicating that these filters were capturing most of the nanoparticles in suspension. Although the monomer diameters for a portion of the Ag NPs were smaller than the nominal filter pore size, our measurements of hydrodynamic diameters suggested that the particles were somewhat aggregated in their stock suspensions. Moreover the retention of nanoparticles on the filters could have occurred via hydrophobic or electrostatic interactions between particles and the membrane filter.

**Aggregation of NPs in the Presence of Cysteine.** We performed measurements of hydrodynamic diameter to determine if cysteine altered the aggregation rate of Ag NPs. The light intensity-weighted average hydrodynamic diameters in the Ag NP-cysteine mixtures were determined by dynamic light scattering (DLS) (Malvern Zetasizer) using incident light ($\lambda$ = 633 nm) scattered at 173°. Zeta potential was calculated from the electrophoretic mobility of the silver nanoparticles measured in triplicate at 25 °C (Malvern Zetasizer). The average hydrodynamic diameter $a_h$ was monitored over time until it reached twice the initial diameter. In cases where aggregation was too slow, $a_h$ was monitored up to 48 h. Observed aggregation rates, $(da_h/dt)_{t\to 0}$ were calculated in a manner similar to previously described methodologies[39−41] in which early stage aggregation rates were approximated by the slope of the linear least-squares regression of data plotted as $a_h$ versus time.

Aggregation experiments were replicated 2−9 times, as determined by a relative standard deviation less than 25% for replicate measurements of $(da_h/dt)_{t\to 0}$. Aggregation rates were quantified in suspensions containing a range of electrolyte concentration (10−1000 mM $NaNO_3$).

**Silver Speciation of Ag NPs.** The speciation of silver particles that collected on the membrane filters was assessed using silver $L_{III}$-edge X-ray absorption near edge spectroscopy (XANES). The Ag $L_{III}$-edge XANES can be used to study the oxidation state and speciation of silver due to a prominent peak exhibited by the spectra at the absorption edge.[42] For each Ag NP-CYS mixture, approximately 100 mL of sample was passed through the 0.025-$\mu$m filters. The filter membrane was stored at −20 °C for 1 hour, freeze-dried, and stored in a desiccator before analysis.

Reference materials for XANES data analysis included PVP- and citrate-coated Ag NPs collected on the membrane filters directly from their stock suspensions. Reference materials for monovalent forms of silver included Ag(+I)-cysteine powders formulated with 1:1 and 1:2 silver/cysteine molar ratios (Ag(CYS) and $Ag(CYS)_2$), Ag-citrate, and commercially purchased powders of $AgNO_{3(s)}$, AgCl, $Ag_2O$, and $Ag_2S$. The SI contains details regarding the preparation of these reference samples.

XANES spectra for the samples were collected at room temperature in fluorescence mode at the Stanford Synchrotron Radiation Lightsource (SSRL) wiggler beamline 4−3. The energy was tuned using a liquid $N_2$ cooled Si(111) $\varphi$ = 90°, unfocused, monochromator crystal. Background subtraction and normalization of spectra were performed using the Athena software package following previous procedures.[43] Linear combination fitting (LCF) of XANES data for the Ag NP +cysteine samples was performed by fitting a binary mixture of reference spectra in the range 20 eV below and above the Ag $L_{III}$-edge (3351 eV). The relative proportions and the errors were determined by the software's least-squares fitting module. Best fits were considered the ones with the lowest R-factor, $\chi^2$, and $\Delta\chi^2$, which are fitting residual parameters described further in the SI.

## RESULTS AND DISCUSSION

**Dissolution of Ag NPs Exposed to Cysteine.** In our batch experiments, the presence of cysteine not only increased the amount of dissolved silver released from Ag-CIT and Ag-PVP nanoparticles, but the cysteine also appeared to modify the surface composition and aggregation rates. In the absence of CYS, the nominally dissolved silver concentration in the diluted Ag-CIT and Ag-PVP suspensions was less than 10% of the total silver. However, in the presence of 400 $\mu$M CYS (in Ag NP mixtures containing 7.6−8 $\mu$M total Ag), the amount of silver passing through the 0.025-$\mu$m filter increased within the first 12 h and appeared to reach a maximum concentration in 24−48 h (Figure 1). At the 48 h time point, the concentration of silver in the filtered fraction was 36.4 ± 2.2% of total silver for Ag-CIT and 47 ± 5.6% for Ag-PVP. When Ag NPs were exposed to

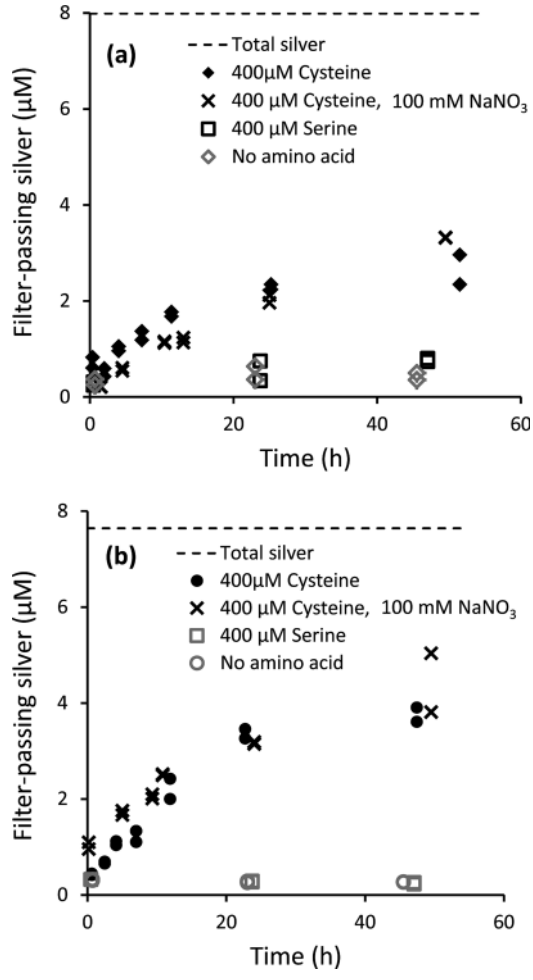


**Figure 1.** Concentration of silver passing through a 0.025-$\mu$m filter in mixtures of (a) Ag-CIT and (b) Ag-PVP nanoparticles suspended in solutions containing 7 mM $NaHCO_3$, 10 mM $NaNO_3$, and either 400 $\mu$M cysteine, 400 $\mu$M serine, or no amino acid. The Ag NP-cysteine experiments were also performed in 100 mM $NaNO_3$. For all solutions, the pH was 7.5−8.1. Total silver concentrations measured in unfiltered samples are indicated by dashed lines.


dx.doi.org/10.1021/es3001757 | Environ. Sci. Technol. 2012, 46, 7037−7045

**Table 1. Initial Dissolution Rates of Ag-PVP and Ag-CIT Solutions Containing 400 $\mu$M CYS and 10 mM $NaNO_3$ (Stable Suspension) or 100 mM $NaNO_3$ (Fast Aggregating)[a]**

| type of Ag NP | total Ag ($\mu$M) | $NaNO_3$ (mM) | surface area per volume of sample ($m^2\ L^{-1}$) | silver dissolution rate ($\mu M\ h^{-1}$) | surface area-normalized dissolution rate ($\mu mol\ m^{-2}\ h^{-1}$) |
|---|---|---|---|---|---|
| Ag-CIT | 8.0 | 10 | $13.9\ (\pm 3.9) \times 10^{-3}$ | 0.10 ± 0.013 | 7.2 ± 2.2 |
| | 8.0 | 100 | $13.9\ (\pm 3.9) \times 10^{-3}$ | 0.087 ± 0.0073 | 6.3 ± 1.8 |
| Ag-PVP | 7.6 | 10 | $54.3\ (\pm 5.7) \times 10^{-3}$ | 0.15 ± 0.013 | 2.8 ± 0.38 |
| | 7.6 | 100 | $54.3\ (\pm 5.7) \times 10^{-3}$ | 0.13 ± 0.011 | 2.4 ± 0.32 |
| | 2.0 | 10 | $14.3\ (\pm 1.5) \times 10^{-3}$ | 0.037 ± 0.0024 | 2.6 ± 0.32 |

[a]Rates were also normalized to the total surface area of particles at the initial time point. The dissolution rates for 100 mM $NaNO_3$ demonstrated statistically significant differences ($p < 0.05$) relative to the corresponding dissolution rates in 10 mM $NaNO_3$ (for mixtures with 8.0 or 7.6 $\mu$M total Ag).

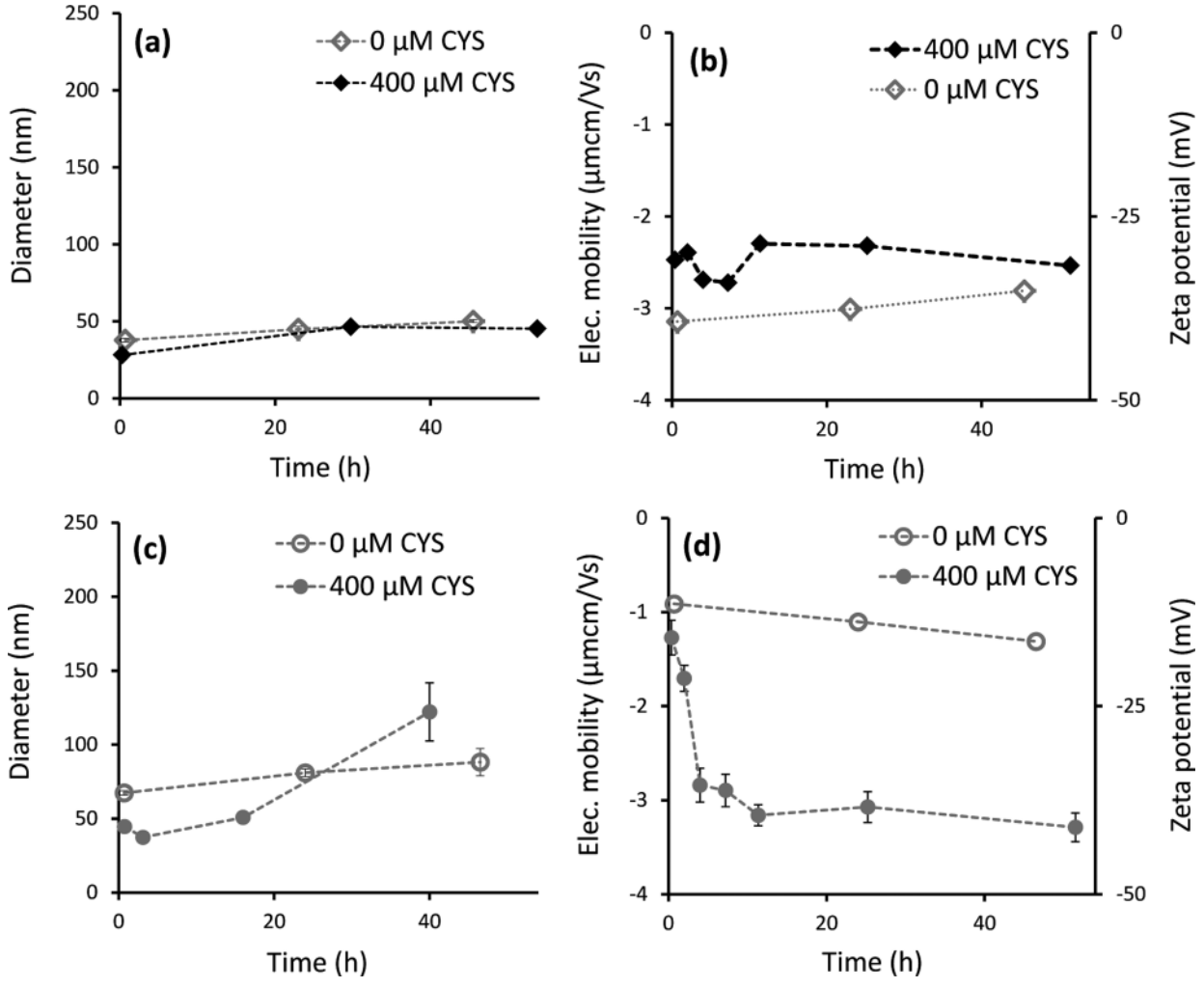


**Figure 2.** Average hydrodynamic diameter and electrophoretic mobility: (a) and (b) Ag-CIT nanoparticles (8.0 $\mu$M total silver); (c) and (d) Ag-PVP nanoparticles (7.6 $\mu$M total silver). The nanoparticles were suspended in mixtures consisting of 7 mM $NaHCO_3$, 10 mM $NaNO_3$, and either 400 $\mu$M CYS or no amino acid. Error bars indicate standard deviations of duplicate diameter measurements and triplicate electrophoretic mobility measurements.

serine instead of cysteine, the filter-passing silver concentration was similar to the control without any amino acids (Figure 1), suggesting that Ag−thiolate interactions were important for Ag dissolution.

Our results contrast a previous study[44] in which Liu et al. reported that thiols, including CYS, inhibited the release of dissolved Ag from Ag NPs. These contradictory results likely stem from differences in experimental methodology. For example, our control experiments indicated that our method of filtration separated dissolved silver from particulate, while the centrifugal ultrafilters (utilized by Liu et al.) have been reported to retain significant amounts of dissolved silver in certain conditions.[45] In addition, cysteine is capable of forming polymers/particles with Ag(+I),[25,46] particularly at low ratios of cysteine/silver (e.g., 5 or less in our mixtures, Figure S2). We did not observe the formation of particulate silver for cysteine:silver molar ratio of 50. Therefore, in this study we

formulated our Ag NP-cysteine mixtures with this ratio to prevent the formation of Ag-CYS particles.

The silver content in the filtered samples is likely to comprise mainly of dissolved Ag released from the nanoparticles. A proportion of this silver could also be small Ag NPs (smaller than the original NPs) that also passed through the filters; however, the dynamic light scattering data do not indicate a predominance of very small particles in solution. Hydrodynamic diameters of the suspensions were increasing in most mixtures with cysteine (discussed in the next section).

Assuming that the filter-passing silver in the first 12 h of data in Figure 1 represented dissolved Ag, we calculated an observed initial dissolution rate by estimating the slope of the data using a linear regression. The error for these rates was estimated as one standard deviation of the slope. In the presence of cysteine and 10 mM $NaNO_3$, the initial dissolution rate of Ag-PVP was 0.15 ± 0.013 $\mu$M/h, which was greater than the corresponding dissolution rate for Ag-CIT (0.10 ± 0.013 $\mu$M/h) (Table 1).

Surface area can be a limiting factor for dissolution of sample constituents.[47,48] From the specific surface areas of the original Ag NPs, we calculated that the surface area-normalized dissolution rate was 2.8 ± 0.38 $\mu$mol $m^{-2}$ $h^{-1}$ for the Ag-PVP and 7.2 ± 2.2 $\mu$mol $m^{-2}$ $h^{-1}$ for the Ag-CIT (both with 10 mM $NaNO_3$) (Table 1). The Ag-PVP dissolution experiment was repeated with 2.0 $\mu$M total Ag, which corresponded to approximately the same total surface area ($14 \times 10^{-3}$ $m^2$ $L^{-1}$) as the samples with 8 $\mu$M Ag-CIT (Table 1 and Figure S3). The dissolution rate for Ag-PVP (2.6 ± 0.32 $\mu$mol $m^{-2}$ $h^{-1}$) was still less than for Ag-CIT.

Although the surface area-normalized initial dissolution rate was slower in the case of Ag-PVP, the relative proportion of silver that was released into solution after 48 h was greater in the Ag-PVP mixtures than the Ag-CIT mixtures (47 ± 5.6% and 36 ± 2.2%, respectively). One possible explanation for this difference is that the relative "accessibility" of particle surfaces for cysteine molecules was lower for Ag-PVP particles than for Ag-CIT, resulting in slower dissolution rates for the Ag-PVP particles. Although we have no direct evidence to demonstrate this phenomenon, we observed a similar indication that reactions at the surface of PVP-coated nanoparticles were relatively slow in aggregation experiments (Figure S4). Here, the aggregation of PVP-coated Ag NPs exhibited an initial lag period ranging from 10 to 50 min, during which the hydrodynamic diameters of the particles were constant. After this lag period, the diameters increased linearly with time. No lag period was observed with the citrate-coated nanoparticles.

**Aggregation and Zeta Potential of Ag NPs Exposed to Cysteine.** The presence of cysteine in the Ag NP suspensions not only increased the dissolution rate of Ag from the nanomaterials, but also altered the aggregation rate and electrophoretic mobility of the particles in suspensions (Figures 2 and 3). In the same Ag NP mixtures corresponding to our dissolved Ag data (Figure 1), the Ag-CIT and Ag-PVP nanoparticles aggregated slightly over 48 h in the absence of CYS (Figure 2a and 2c, respectively).

With the addition of CYS in the Ag-CIT suspensions (with 10 mM $NaNO_3$), the hydrodynamic diameter did not change relative to samples without CYS (Figure 2a). In the Ag-PVP mixtures, the average hydrodynamic diameters at the initial time point decreased from 67 nm in the absence of CYS to 45 nm in the presence of CYS. The decrease in Ag-PVP diameter due to CYS exposure was potentially caused by disaggregation of aggregates in the nanoparticle stock or perhaps by the

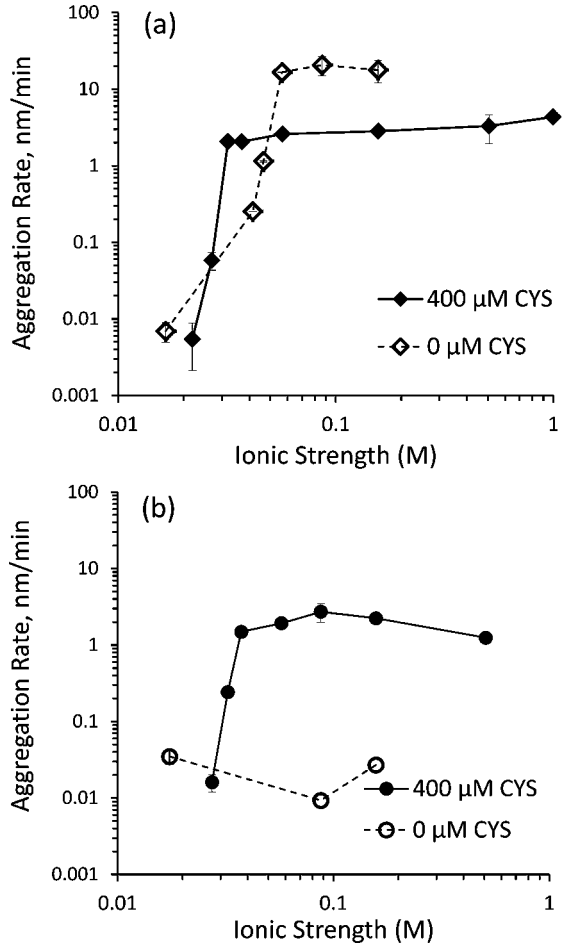


**Figure 3.** Initial aggregation rate of silver nanoparticles in bicarbonate solutions (a) Ag-CIT (8.0 $\mu$M total silver) and (b) Ag-PVP (7.6 $\mu$M total silver) in suspensions comprising 7 mM $NaHCO_3$ and 400 $\mu$M CYS at pH values between 7.5 and 8.1. In some experiments no cysteine was added. Ionic strength was controlled with the addition of $NaNO_3$ at concentrations ranging from 0.01 to 1 M.

replacement of PVP (a long chain polymer with an average molecular weight of 55 000 Da) with CYS (a small amino acid with molecular weight 121 Da) on the surface of the nanoparticles. For the nanoparticles stabilized with citrate (a low molecular weight coating relative to PVP), the influence of CYS on hydrodynamic diameter at the initial time point was not as drastic.

The zeta potential of Ag-CIT particles increased from −37.6 to −29.0 mV (at 24 h) in the presence of 400 $\mu$M CYS (Figure 2b). The measurement uncertainty may be up to 15%, but the net increase in zeta potential could be due to the exchange of the trivalent citrate anion for the monovalent cysteine anion (at pH 7.5) on the surface of the Ag-CIT nanoparticles. In contrast, the zeta potential of Ag-PVP particles without CYS was −13.8 mV (after 24 h in solution, Figure 2d). This zeta potential suggests a surface charge that is closer to neutral compared to the Ag-CIT nanoparticles, yet little aggregation was observed for the Ag-PVP suspensions (without CYS). This observation suggests that the PVP coating mainly provides steric (rather than electrostatic) stabilization for the nanoparticles. When the Ag-PVP nanoparticles were exposed to CYS, the zeta potential of those particles at 24 h was −38.4 mV (Figure 2d), possibly due to sorption of cysteine anions. For


dx.doi.org/10.1021/es3001757 | Environ. Sci. Technol. 2012, 46, 7037−7045

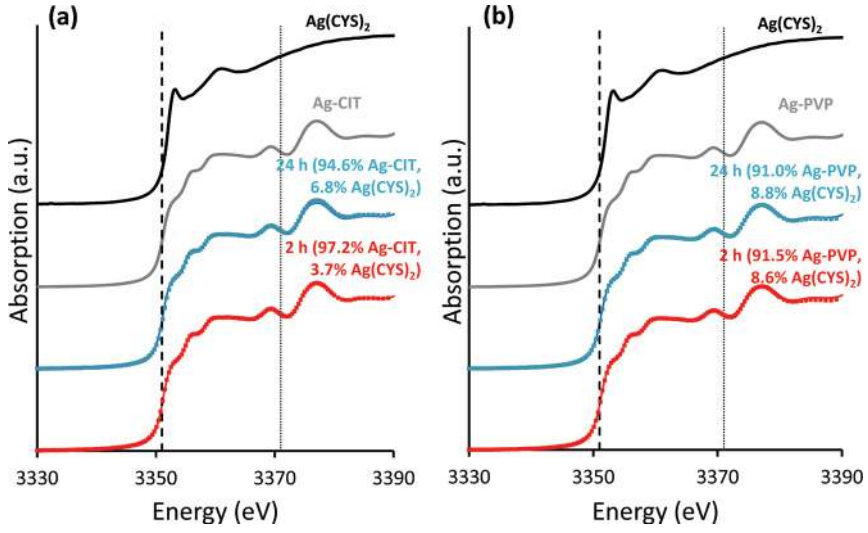


**Figure 4.** Normalized silver $L_{III}$-edge XANES spectra of the original Ag NPs, Ag(+I)-cysteine complexes $Ag(CYS)_2$, and silver nanoparticles that were exposed to cysteine for 2 or 24 h: (a) Ag-CIT; (b) Ag-PVP. The nanoparticles (8.0 $\mu$M total silver in Ag-CIT and 7.6 $\mu$M in Ag-PVP samples) were exposed to 400 $\mu$M CYS in mixtures containing 7 mM $NaHCO_3$, 10 mM $NaNO_3$, and pH 7.5−8.1. After this exposure period, the particles were collected on filter membranes for XANES analysis. The data points correspond to linear combination fits for spectra of the original Ag NPs and $Ag(CYS)_2$ reference material.

**Table 2. Linear Combination Fitting Results of XANES Spectra for Ag-CIT and Ag-PVP Nanoparticles Exposed to Cysteine in Solutions Containing 7 mM $NaHCO_3$ and 10 mM $NaNO_3$, and at pH 7.5−8.1[a]**

| sample | % Ag NP | % $Ag(CYS)_2$ | $R$ | $\chi^2$ | $\Delta\chi^2$ |
|---|---|---|---|---|---|
| Ag-CIT + CYS (2 h) | 97.2 (±0.9) | 3.7 (±0.8) | $5.3 \times 10^{-5}$ | $18.1 \times 10^{-4}$ | $16.0 \times 10^{-6}$ |
| Ag-CIT + CYS (24 h) | 94.6 (±1.4) | 6.8 (±1.2) | $11.7 \times 10^{-5}$ | $40.3 \times 10^{-4}$ | $35.7 \times 10^{-6}$ |
| Ag-PVP + CYS (2 h) | 91.9 (±0.8) | 7.2 (±0.7) | $3.8 \times 10^{-5}$ | $12.7 \times 10^{-4}$ | $11.3 \times 10^{-6}$ |
| Ag-PVP + CYS (24 h) | 91.3 (±0.4) | 7.9 (±0.3) | $1.0 \times 10^{-5}$ | $3.3 \times 10^{-4}$ | $2.9 \times 10^{-6}$ |

[a]Energy range −20 to +20 eV from the Ag $L_{III}$-edge (3351 eV) in the XANES spectra was used for the model fits to reference spectra of the silver nanoparticles (without modification) and the reference sample of the 1:2 Ag(+I)−cysteine complex. Standard deviations of the model fits are shown in parentheses.

both types of Ag NPs, the zeta potential data indicated that CYS was modifying the surface of the nanoparticles, potentially by sorbing to the surface and by replacing the initial citrate and PVP coatings.

At a relatively low ionic strength (10 mM $NaNO_3$), the presence of cysteine had a small effect on aggregation relative to samples without cysteine (Figure 2). At higher $NaNO_3$ concentrations (up to 1000 mM), the presence of cysteine appeared to destabilize both Ag-PVP and Ag-CIT suspensions (Figure 3). For example, the critical coagulation concentrations (ccc) for the Ag-CIT suspensions decreased from 53 ± 5.3 mM in the absence of CYS to 35 ± 2.2 mM in the presence of 400 $\mu$M CYS (Figure 3a). The decrease in ccc was consistent with electrophoretic mobility measurements showing that CYS induced a net shift toward neutral surface charge for the particles (Figure 2b).

The Ag-PVP suspensions (without CYS) did not aggregate appreciably within 48 h in solutions containing a large range of ionic strength values (from 10 to 1000 mM $NaNO_3$) (Figure 3b). The presence of CYS in the Ag-PVP suspensions caused the particles to aggregate, particularly at high ionic strength values (i.e., greater than 20 mM). Based on the observed aggregation rates, we estimated a ccc value of 33 ± 5.3 mM for Ag-PVP particles in the presence of CYS (Figure 3b). The observations that CYS induced aggregation (rather than inhibited aggregation) was inconsistent with observed changes in zeta potential, which decreased to more negative values when CYS was present (Figure 2d). Rather, we hypothesize that the interaction between CYS and the surface of the PVP-coated nanoparticles resulted in loss of steric repulsive forces enabled by the PVP.

**Effect of Aggregation on Dissolution.** Aggregation of the nanoparticles is expected to change the amount of available surface area for surface reactions such as dissolution. Thus, we compared how initial dissolution rates changed for suspensions that were relatively stable (10 mM $NaNO_3$) and suspensions of fast aggregating particles (Figure S5) with an ionic strength value (100 mM) greater than the ccc for both nanoparticles. For both Ag-CIT and Ag-PVP, the initial dissolution rates of the fast aggregating samples appeared to be lower than in stable suspensions (Table 1, Figure 2). Although the error of the measurements indicated an overlapping range of rates, the differences in dissolution rates at low (10 mM) and high ionic strength (100 mM) were statistically significant ($p$-values of <0.001 and 0.022 for the Ag-CIT and Ag-PVP, respectively). This difference could be caused by a decrease in reactive surface area as the particles aggregated. The difference in dissolution rates at low and high ionic strength could also be explained by smaller nanoparticles that remained unaggregated (in low ionic strength) and were small enough to pass through the filters.

**Speciation of Particulate Silver.** XANES analysis was used to determine the oxidation state and speciation of particulate silver in samples containing Ag NPs and cysteine (Figure 4 and Figure S6). Linear combination fitting (LCF) of

the spectra was performed assuming a binary mixture of the original nanomaterial (Ag-CIT or Ag-PVP) and one of the Ag(+I) reference compounds (Table 2 and Tables S1−S4). LCF attempts using ternary combinations of reference spectra did not improve the quality of fits; thus, we do not show these results. The XANES analysis indicated that up to 10% of silver in the particles was oxidized to Ag(+I) and coordinated to reduced sulfur, as compared to the original oxidation state of each respective particle suspension. Fitting with several silver−sulfur references such as $Ag_2S$, Ag(CYS), and $Ag(CYS)_2$ yielded very similar values of R-factor, $\chi^2$, and $\Delta\chi^2$, indicating that the nature of the bond between silver and sulfur could be similar to one or a combination of these references. We selected fits with $Ag(CYS)_2$ as the representative silver−sulfur model compound for further comparisons between the Ag NP-CYS mixtures (Table 2 and Figure 4).

Ag-PVP particles that were exposed to CYS exhibited a higher percentage of oxidized silver (7.2% and 7.9% at 2 h and 24 h) than Ag-CIT (3.7% and 6.8%, respectively) (Table 2). This observation could be explained by our results that the Ag-PVP particles were smaller than Ag-CIT and would comprise a greater proportion of silver atoms at the particle surface.[48] We note that relative differences of a few percentages in XANES modeling must be interpreted carefully. The relatively smaller errors reported from the fitting software (shown in Table 2) do suggest a difference in the amount of oxidized silver for the Ag-CIT and Ag-PVP samples. However, in previous XANES studies that used LCF for known sample mixtures,[49] the results of mixing ratios showed that the error from LCF calculations can be up to ±5%.

Overall, our interpretation of the XANES data suggested that a portion of the silver atoms (presumably on the surface of the Ag NPs) were in the monovalent oxidation state and were coordinated to reduced sulfur (either cysteine or sulfide).

**Cysteine Adsorption.** Cysteine was also quantified in the filtered Ag NP+CYS mixtures. The results showed that dissolved cysteine decreased within 48 h in both nanoparticle samples (Figure S7a). A larger decrease of dissolved cysteine was observed in the Ag-PVP suspensions than in the Ag-CIT suspensions. This difference was potentially due to the larger specific surface area of the Ag-PVP particles relative to Ag-CIT particles. To test this hypothesis, we calculated the change in dissolved cysteine concentration (relative to the initial concentration) and normalized these values to the total initial surface area of Ag NPs (Figure S7b). For both types of nanomaterials, the changes in dissolved cysteine concentrations were approximately 1−2 mmol per $m^2$ of NP after 48 h of mixing. Based on the errors (propagated from the CYS measurements), there were no apparent differences between Ag NPs (Figure S7b).

Although the loss of dissolved cysteine could be interpreted as adsorption to the Ag NPs, the amount of cysteine lost (31 and 96 $\mu$M) was greater than the total Ag silver concentration in suspensions (~8 $\mu$M). Thus, sorption would not fully explain the loss of dissolved cysteine. Control experiments with cysteine in the buffer solution without Ag NPs were performed to determine if cysteine would oxidize under the experimental conditions. In this experiment, we quantified a loss of approximately 25 $\mu$M dissolved cysteine in a 48 h period (Figure S7a). This amount of cysteine oxidation is close to the decrease of dissolved cysteine in the Ag-CIT mixture (31 $\mu$M), but did not fully account for the loss of dissolved cysteine (96 $\mu$M) in the Ag-PVP mixture. Other reactions at the surface of the PVP-coated Ag NPs, such as the production of reactive oxygen species from $O_2$ (e.g., superoxide, hydrogen peroxide, hydroxyl radicals) as the silver nanoparticles oxidize and dissolve, may subsequently react with and oxidize cysteine. Although dissolved $O_2$ appears to be a necessary electron acceptor for oxidative dissolution of silver nanoparticles,[18] we have no knowledge of direct evidence for the production of reactive oxygen species during this process, and further study is needed to understand the reaction products of oxidative dissolution of Ag NPs.

**Environmental Significance.** This study highlights the multiple transformations that can occur when silver nanoparticles are exposed to Ag-binding ligands that can modify the surface composition of the particles and their aggregation and dissolution rates. In our experiments, cysteine increased the solubility of the particles; however, the dissolution rate depended on the aggregation state of the particles and surface modifications caused by sorption of cysteine. All of these processes (surface modifications, aggregation, and dissolution) work in concert to influence the overall persistence and composition of the silver nanomaterials in aqueous suspension. Furthermore, these simultaneous transformations could alter the bioavailability of the nanomaterials to exposed organisms. For example, the presence of $Ag^+$-binding ligands is expected to increase the amount of dissolved Ag that can be internalized by aquatic organisms; however, the rate of dissolution would depend on the aggregation state of the particles and surface modifications by the ligand. Furthermore, previous studies have shown that cysteine and other low molecular weight thiols can reduce silver toxicity to organisms exposed to silver nanomaterials.[30] Although complexation of dissolved $Ag^+$ by cysteine is the likely mode of action (due to the relatively strong affinity between $Ag^+$ and cysteine), our results indicated that cysteine can also induce aggregation of the nanomaterials, leading to a secondary mechanism by which the presence of cysteine could decrease Ag NP toxicity.

The transformations discussed in our study appeared to take place on the surface of particles, which were originally coated with PVP or citrate. Nanomaterials are typically manufactured with organic coatings that serve to stabilize the suspension during production. In this work we demonstrated that the dissolution rates of PVP-coated particles (when normalized to the specific surface area) were slower than those of citrate-coated particles. One possible explanation for this phenomenon is that diffusion of cysteine molecules at the particle−water interface of PVP-coated nanoparticles is slower than diffusion at the interfacial region of citrate-coated nanoparticles. Another possible explanation is that dissolved citrate (carried over from the stock solution) is capable of binding $Ag^+$, resulting in additional free cysteine molecules that are able to associate with particle surfaces and dissolve the particles. Overall our results demonstrate the importance of the synthetic coatings for the reactivity of Ag NPs.

Cysteine was used in this study as an example of thiol-containing organic ligands that are ubiquitous in the aquatic environment.[50,51] The fact that serine did not cause similar effects indicated the importance of strong $Ag^+$-binding ligands (i.e., thiols) for interactions with Ag NPs. Cysteine can be found in nanomolar concentrations in natural waters[21] (e.g., sediment porewater, surface waters, and wastewater) and is also a component of complex organic structures, such as proteins and natural organic matter (NOM). In these waters, the concentration of all thiol-containing ligands (up to micromolar

quantities) would be higher than the expected concentrations for Ag NPs.[21−25] Such observations have been made in previous studies investigating wastewater containing silver contamination derived from the photographic industry.[52]

Our study indicated that Ag NPs were altered by cysteine, but further research is needed to demonstrate whether cysteine will have the same effects on Ag NPs when the ligand is part of a more complex structure such as proteins or NOM. Steric effects are expected to occur with macromolecular structures and may alter the rates of reactions between thiolate functional groups and the surface of Ag. Recent studies have indicated that molecular weight and aromaticity of NOM are more important properties than reduced sulfur content in determining the dissolution of HgS cinnabar particles and the precipitation and aggregation of ZnS nanoparticles.[53,54] Future studies could consider the macromolecular structure of more complex "ligands" such as humic substances, particularly as they influence simultaneous transformations of the Ag NPs (aggregation, dissolution, surface reactivity) and bioavailability to exposed organisms.

## ■ ASSOCIATED CONTENT

### Supporting Information

TEM images of Ag NPs, results of filtration for dissolution control experiments, examples of hydrodynamic diameter measurements for aggregation experiments, description of sample preparation for XANES analysis, the XANES spectra, and LCF results. This information is available free of charge via the Internet at http://pubs.acs.org/.

## ■ AUTHOR INFORMATION

### Corresponding Author

*Phone (919) 660-5109; e-mail: hsukim@duke.edu.

### Notes

The authors declare no competing financial interest.

## ■ ACKNOWLEDGMENTS

We thank Jeff Farner Budarz for his help with experiments, Yingwen Cheng for preparing the Ag-PVP suspension, and Armand Masion for his valuable advice. We also thank beamline scientists Matthew Latimer and Erik Nelson at SSRL. This material is based upon work supported by the National Science Foundation (NSF) and the Environmental Protection Agency (EPA) under NSF Cooperative Agreement EF-0830093, Center for the Environmental Implications of NanoTechnology (CEINT). Any opinions, findings, conclusions or recommendations expressed in this material are those of the authors and do not necessarily reflect the views of NSF or EPA. This work has not been subjected to EPA review and no official endorsement should be inferred. A.G. was also supported by the Greek Scholarships Foundation.

## ■ REFERENCES

(1) Wiesner, M. R.; Lowry, G. V.; Alvarez, P.; Dionysiou, D.; Biswas, P. Assessing the risks of manufactured nanomaterials. *Environ. Sci. Technol.* **2006**, *40* (14), 4336−4345.

(2) Wiesner, M. R.; Lowry, G. V.; Jones, K. L.; Hochella, M. F.; Di Giulio, R. T.; Casman, E.; Bernhardt, E. S. Decreasing uncertainties in assessing environmental exposure, risk, and ecological implications of nanomaterials. *Environ. Sci. Technol.* **2009**, *43* (17), 6458−6462.

(3) Narkis, N.; Rebhun, M. The mechanism of flocculation processes in the presence of humic substances. *J. Am. Water Works Assoc.* **1975**, 101−108.

(4) Mylon, S. E.; Chen, K. L.; Elimelech, M. Influence of natural organic matter and ionic composition on the kinetics and structure of hematite colloid aggregation: Implications to iron depletion in estuaries. *Langmuir* **2004**, *20*, 9000−9006.

(5) Gondikas, A. P.; Jang, E. K.; Hsu-Kim, H. Influence of amino acids cysteine and serine on aggregation kinetics of zinc and mercury sulfide colloids. *J. Colloid Interface Sci.* **2010**, *347* (2), 167−171.

(6) Vikesland, P. J.; Heathcock, A. M.; Rebodos, R. L.; Makus, K. E. Particle size and aggregation effects on magnetite reactivity toward carbon tetrachloride. *Environ. Sci. Technol.* **2007**, *41* (15), 5277−5283.

(7) Liu, J.; Aruguete, D. M.; Murayama, M.; Hochella, M. F. Influence of size and aggregation on the reactivity of an environmentally and industrially relevant nanomaterial (PbS). *Environ. Sci. Technol.* **2009**, *43*, 8178−8183.

(8) Barton, L. E.; Grant, K. E.; Kosel, T.; Quicksall, A. N.; Maurice, P. A. Size-dependent Pb sorption to nanohematite in the presence and absence of a microbial siderophore. *Environ. Sci. Technol.* **2011**, *45* (8), 3231−3237.

(9) Andren, A.; Bober, T. W. *Silver in the Environment: Transport, Fate, and Effects*; SETAC Press: Pensacola, FL, 2002; pp xxii, 169.

(10) Pearson, R. G. Hard and soft acids and bases. *J. Am. Chem. Soc.* **1963**, *85* (22), 3533−3539.

(11) Kramer, J. R.; Adams, N. W. H.; Manolopoulos, H.; Collins, P. V. Silver at an old mining camp, Cobalt, Ontario, Canada. *Environ. Toxicol. Chem.* **1999**, *18* (1), 23−29.

(12) Kramer, J. R.; Adams, N. W. H. Silver speciation in wastewater effluent, surface waters, and pore waters. *Environ. Toxicol. Chem.* **1999**, *18* (12), 2667−2673.

(13) Miller, L. A.; Bruland, K. W. Organic speciation of silver in marine waters. *Environ. Sci. Technol.* **1995**, *29* (10), 2616−2621.

(14) Reinsch, B. C.; Levard, C.; Li, Z.; Ma, R.; Wise, A.; Gregory, K. B.; Brown, G. E.; Lowry, G. V. Sulfidation of silver nanoparticles decreases *Escherichia coli* growth inhibition. *Environ. Sci. Technol.* **2012**, DOI: 10.1021/es203732x.

(15) Ma, R.; Levard, C.; Marinakos, S. M.; Cheng, Y.; Liu, J.; Michel, F. M.; Brown, G. E.; Lowry, G. V. Size-controlled dissolution of organic-coated silver nanoparticles. *Environ. Sci. Technol.* **2012**, *46*, 752−759.

(16) Li, X. A.; Lenhart, J. J.; Walker, H. W. Dissolution-accompanied aggregation kinetics of silver nanoparticles. *Langmuir* **2010**, *26* (22), 16690−16698.

(17) Levard, C.; Reinsch, B. C.; Michel, F. M.; Oumahi, C.; Lowry, G. V.; Brown, G. E. Sulfidation processes of PVP-coated silver nanoparticles in aqueous solution: Impact on dissolution rate. *Environ. Sci. Technol.* **2011**, *45* (12), 5260−5266.

(18) Liu, J. Y.; Pennell, K. G.; Hurt, R. H. Kinetics and mechanisms of nanosilver oxysulfidation. *Environ. Sci. Technol.* **2011**, *45* (17), 7345−7353.

(19) Kaegi, R.; Voegelin, A.; Sinnet, B.; Zuleeg, S.; Hagendorfer, H.; Burkhardt, M.; Siegrist, H. Behavior of metallic silver nanoparticles in a pilot wastewater treatment plant. *Environ. Sci. Technol.* **2011**, *45* (9), 3902−3908.

(20) Adams, N. W. H.; Kramer, J. R. Reactivity of Ag+ ion with thiol ligands in the presence of iron sulfide. *Environ. Toxicol. Chem.* **1998**, *17* (4), 625−629.

(21) Shea, D.; Maccrehan, W. A. Determination of hydrophilic thiols in sediment porewater using ion-pair liquid-chromatography coupled to electrochemical detection. *Anal. Chem.* **1988**, *60* (14), 1449−1454.

(22) Ciglenecki, I.; Cosovic, B.; Vojvodic, V.; Plavsic, M.; Furic, K.; Minacci, A.; Baldi, F. The role of reduced sulfur species in the coalescence of polysaccharides in the Adriatic Sea. *Mar. Chem.* **2000**, *71* (3−4), 233−249.

(23) Ahner, B. A.; Kong, S.; Morel, F. M. M. Phytochelatin production in marine algae. 2. Induction by various metals. *Limnol. Oceanogr.* **1995**, *40* (4), 658−665.

(24) Le Faucheur, S.; Behra, R.; Sigg, L. Thiol and metal contents in periphyton exposed to elevated copper and zinc concentrations: A field and microcosm study. *Environ. Sci. Technol.* **2005**, *39* (20), 8099−107.

(25) Bell, R.; Kramer, J. Structural chemistry and geochemistry of silver-sulfur compounds: Critical review. *Environ. Toxicol. Chem.* **1999**, *18* (1), 9−22.
(26) Fahey, R. C.; Brown, W. C.; Adams, W. B.; Worsham, M. B. Occurrence of glutathione in bacteria. *J. Bacteriol.* **1978**, *133* (3), 1126−9.
(27) Ellman, G. L. Tissue sulfhydryl groups. *Arch. Biochem. Biophys.* **1959**, *82* (1), 70−77.
(28) Lau, B. L. T.; Hsu-Kim, H. Precipitation and growth of zinc sulfide nanoparticles in the presence of thiol-containing natural organic ligands. *Environ. Sci. Technol.* **2008**, *42* (19), 7236−7241.
(29) Deonarine, A.; Hsu-Kim, H. Precipitation of mercuric sulfide nanoparticles in NOM-containing water: Implications for the natural environment. *Environ. Sci. Technol.* **2009**, *43* (7), 2368−2373.
(30) Navarro, E.; Piccapietra, F.; Wagner, B.; Marconi, F.; Kaegi, R.; Odzak, N.; Sigg, L.; Behra, R. Toxicity of silver nanoparticles to *Chlamydomonas reinhardtii*. *Environ. Sci. Technol.* **2008**, *42* (23), 8959−8964.
(31) Miao, A. J.; Schwehr, K. A.; Xu, C.; Zhang, S. J.; Luo, Z. P.; Quigg, A.; Santschi, P. H. The algal toxicity of silver engineered nanoparticles and detoxification by exopolymeric substances. *Environ. Pollut.* **2009**, *157* (11), 3034−3041.
(32) Kawata, K.; Osawa, M.; Okabe, S. In vitro toxicity of silver nanoparticles at noncytotoxic doses to HepG2 human hepatoma cells. *Environ. Sci. Technol.* **2009**, *43* (15), 6046−6051.
(33) Yang, X.; Gondikas, A. P.; Marinakos, S. M.; Auffan, M.; Liu, J.; Hsu-Kim, H.; Meyer, J. N. Mechanism of silver nanoparticle toxicity is dependent on dissolved silver and surface coating in *Caenorhabditis elegans*. *Environ. Sci. Technol.* **2012**, *46*, 1119−1127.
(34) Meyer, J. N.; Lord, C. A.; Yang, X. Y. Y.; Turner, E. A.; Badireddy, A. R.; Marinakos, S. M.; Chilkoti, A.; Wiesner, M. R.; Auffan, M. Intracellular uptake and associated toxicity of silver nanoparticles in *Caenorhabditis elegans*. *Aquat. Toxicol.* **2010**, *100* (2), 140−150.
(35) Liu, J.; Cheng, Y. W.; Yin, L. Y.; Lin, S. H.; Wiesner, M.; Bernhardt, E. Toxicity reduction of polymer-stabilized silver nanoparticles by sunlight. *J. Phys. Chem. C* **2011**, *115* (11), 4425−4432.
(36) Davey, W. P. Precision measurements of the lattice constants of twelve common metals. *Phys. Rev.* **1925**, *25* (6), 753−761.
(37) Hsu-Kim, H. Stability of metal−glutathione complexes during oxidation by hydrogen peroxide and Cu(II) catalysis. *Environ. Sci. Technol.* **2007**, *41*, 2338−2342.
(38) Vairavamurthy, A.; Mopper, K. Field method for determination of traces of thiols in natural-waters. *Anal. Chim. Acta* **1990**, *236* (2), 363−370.
(39) Holthoff, H.; Egelhaaf, S. U.; Borkovec, M.; Schurtenberger, P.; Sticher, H. Coagulation rate measurements of colloidal particles by simultaneous static and dynamic light scattering. *Langmuir* **1996**, *12* (23), 5541−5549.
(40) Schudel, M.; Behrens, S. H.; Holthoff, H.; Kretzschmar, R.; Borkovec, M. Absolute aggregation rate constants of hematite particles in aqueous suspensions: A comparison of two different surface morphologies. *J. Colloid Interface Sci.* **1997**, *196*, 241−253.
(41) Grolimund, D.; Elimelech, M.; Borkovec, M. Aggregation and deposition kinetics of mobile colloidal particles in natural porous media. *Colloids Surf., A* **2001**, *191*, 179−188.
(42) Behrens, P. Bonding in silver-oxygen compounds from Ag $L_{III}$ XANES spectroscopy. *Solid State Commun.* **1992**, *81* (3), 235−239.
(43) Ravel, B.; Newville, M. ATHENA, ARTEMIS, HEPHAESTUS: Data analysis for X-ray absorption spectroscopy using IFEFFIT. *J. Synchrotron. Radiat.* **2005**, *12*, 537−541.
(44) Liu, J.; Sonshine, D. A.; Shervani, S.; Hurt, R. H. Controlled release of biologically active silver from nanosilver surfaces. *ACS Nano* **2010**, *4* (11), 6903−13.
(45) Kennedy, A. J.; Hull, M. S.; Bednar, A. J.; Goss, J. D.; Gunter, J. C.; Bouldin, J. L.; Vikesland, P. J.; Steevens, J. A. Fractionating nanosilver: Importance for determining toxicity to aquatic test organisms. *Environ. Sci. Technol.* **2010**, *44* (24), 9571−9577.
(46) Andersson, L.-O. Study of some silver-thiol complexes and polymers - stoichiometry and optical effects. *J. Polym. Sci., Part A: Polym. Chem.* **1972**, *10* (7), 1963−1973.
(47) Liu, J.; Aruguete, D. M.; Jinschek, J. R.; Rimstidt, J. D.; Hochella, M. F. The non-oxidative dissolution of galena nanocrystals: Insights into mineral dissolution rates as a function of grain size, shape, and aggregation state. *Geochim. Cosmochim. Acta* **2008**, *72*, 5984−5996.
(48) Bottero, J. Y.; Auffan, M.; Rose, J.; Mouneyrac, C.; Botta, C.; Labille, J.; Masion, A.; Thill, A.; Chaneac, C. Manufactured metal and metal-oxide nanoparticles: Properties and perturbing mechanisms of their biological activity in ecosystems. *C. R. Geosci.* **2011**, *343* (2−3), 168−176.
(49) Gaur, A.; Shrivastava, B. D.; Joshi, S. K. Copper K-edge XANES of Cu(I) and Cu(II) oxide mixtures. *J. Phys. Conf. Ser.* **2009**, *190* (190 012084), 1−4.
(50) Mopper, K.; Taylor, B. F. Biogeochemical cycling of sulfur - Thiols in coastal marine sediments. *ACS Symp. Ser.* **1986**, *305*, 324−339.
(51) Zhang, J.; Wang, F.; House, J. D.; Page, B. Thiols in wetland interstitial waters and their role in mercury and methymercury speciation. *Limnol. Oceanogr.* **2004**, *49* (6), 2276−2286.
(52) Shafer, M. M.; Overdier, J. T.; Armstrong, D. E. Removal, partitioning, and fate of silver and other metals in wastewater treatment plants and effluent-receiving streams. *Environ. Toxicol. Chem.* **1998**, *17* (4), 630−641.
(53) Waples, J. S.; Nagy, K. L.; Aiken, G. R.; Ryan, J. N. Dissolution of cinnabar (HgS) in the presence of natural organic matter. *Geochim. Cosmochim. Acta* **2005**, *69* (6), 1575−1588.
(54) Deonarine, A.; Lau, B. L. T.; Aiken, G. R.; Ryan, J. N.; Hsu-Kim, H. Effects of humic substances on precipitation and aggregation of zinc sulfide nanoparticles. *Environ. Sci. Technol.* **2011**, *45* (8), 3217−3223.